Theoretical investigation of the longitudinal Hall effect in $SrAs_3$

R. v. Baltz and W. Denk
Institut für Theorie der Kondensierten Materie, Universität, 7500 Karlsruhe, Germany

W. Bauhofer
Materialien der Mikroelektronik, Technische Universität, 2100 Hamburg-Harburg, Germany
(Received 5 March 1993)

The resistivity and Hall coefficients of $SrAs_3$ are calculated for $T=0$ K using different model band structures. The magnitude of the experimentally observed low-temperature values for the first-order longitudinal Hall coefficients (LHE) cannot be reproduced within a single-band model based on a realistic Fermi surface with monoclinic symmetry. An ellipsoidal two-band model, however, yields a quantitative description of the measured LHE. This result strongly supports our earlier assertion that the LHE is essentially a two-band effect.

An unusual first-order longitudinal Hall effect (LHE) has been recently observed for the low-symmetry compounds $SrAs_3$, $CaAs_3$, and $AuTe_2$.[1-3] The geometrical arrangement for a LHE is characterized by a magnetic field **B** parallel either to the current density **j** or the Hall electrical field **E**. According to the action of the Lorentz force, **j**, **B**, and **E** are expected to be mutually perpendicular [the transverse Hall effect (THE)]. However, in crystals of low symmetry, longitudinal components exist which may be even of the same order of magnitude as the THE components. The measured temperature dependence of the LHE coefficients gives strong evidence that the LHE is essentially a two-band effect. In addition, it has been demonstrated by a model calculation for a monoclinic two-band conductor that nonvanishing LHE coefficients are produced by the products of nondiagonal and diagonal conductivity elements (within the monoclinic ac plane) for the two bands involved.[2] It is the purpose of this paper to investigate quantitatively the order of magnitude of the LHE coefficients of $SrAs_3$ based on model band structures which fulfill the requirements of crystal symmetry. We start with a single monoclinic band which fits the measured (hole) Fermi surface.[4] This single-band model yields values for the LHE coefficients much smaller than those observed. By adding an ellipsoidal electron band, the description of the experimental data can be considerably improved, yet a sign discrepancy remains with the LHE coefficients. An almost-perfect description, however, can be obtained with an ellipsoidal band model for both, holes and electrons.

$SrAs_3$ crystallizes in the monoclinic space group $C2/m$, and the unit cell contains two formula units of $SrAs_3$. The orthogonal laboratory system x_1, x_2, and x_3 is oriented to the crystallographic axes c, a, and b with x_1 parallel to c^*, x_2 parallel to a, and x_3 parallel to b. In this notation b is the twofold axis and the monoclinic angle $b=112°$ is between a, and c. a^*, b^*, and c^* denote the reciprocal-lattice vectors with b^* positioned parallel to b, and a^*, and c^* lie in the (a,c) plane forming an angle of 67.1°.[2] The point group $2/m$ (C_{2h}) contains four elements: the identity (E), a π-rotation around x_3 (C_2), reflection on the x_1, x_2 plane (σ_h), and the inversion (i). C_2 and σ_H are the generators of the group, with $i=C_2 o \sigma_H$ and $E=ioi$. In the low-B limit the resistivity tensor can be expanded as

$$\rho_{ij}(B)=\rho_{ij}+\rho_{ijk}B_k+\cdots , \tag{1}$$

where ρ_{ij} is the (polar, rank-two) zero-field resistivity tensor and ρ_{ijk} denotes the (axial, rank-three) Hall tensor. Higher-order terms in (1) will not be considered here. General symmetry considerations and Onsager's relation require that $\rho_{ij}=\rho_{ji}$ is symmetric and $\rho_{ijk}=\rho_{jik}$ is antisymmetric with respect to the first and second indices.[5] For C_{2h} there are four independent resistivity components: ρ_{11}, ρ_{12}, ρ_{22}, and ρ_{33}, i.e., x_1, x_2, and x_3 are in general not the principal axes of the resistivity tensor. The THE is related to the three independent coefficient ρ_{213}, ρ_{132}, and ρ_{321} and the LHE is characterized by ρ_{131} and ρ_{232}.[5,6]

The electronic properties of single crystals of $SrAs_3$ have been studied by investigating the temperature dependence of the electrical conductivity, the Hall effect, and Shubnikov–de Haas (SdH) oscillations.[2,4] At 4.2 K $SrAs_3$ is predominatly p type, as indicated by the positive sign of the high-field transverse Hall coefficients. The periods of the SdH oscillations have been interpreted with an elliptic cross section of the Fermi body in the b^*c^* plane, while the cross section in the a^*c^* plane resembles a parallelogram with rounded corners. A rough estimate of the hole concentration n_h using an ellipsoidal approximation suggests the existence of two equivalent Fermi bodies to reconcile the SdH carrier density with the Hall data. We use $n_h=6.9\times10^{17}$ cm^{-3} as a starting value. A further low-frequency SdH oscillation[4] has been explained by a spherical electron band with $n_e=1.4\times10^{16}$ cm^{-3}. Since no band-structure investigation is available yet, we set up an expansion of $E(k)$ in terms of polynomials in k_1, k_2, and k_3, which are invariant under the group of the wave vector k_0 of the center

of the respective Fermi bodies. In reciprocal space, the orthogonal system k_1, k_2, and k_3 is chosen parallel to x_1, x_2, and x_3 (i.e., parallel to c^*, a, and b). We assume both hole Fermi bodies to be located near the center of the Brillouin zone ($k_0=0$) so that $E(k)$ of each Fermi body is invariant under all point-group transformations, i.e., the generators C_2 and σ_h. These polynomials can be constructed from invariant monoms $x^k y^m z^n$ with $n=$even and $k+m=$even. Therefore, in dimensionless form, the monoclinic hole band is described by

$$\hat{E}(\hat{k})=a\hat{k}_x^2+b\hat{k}_x^4+c\hat{k}_x^6+d\hat{k}_y^2+e\hat{k}_y^4+f\hat{k}_y^6+gk_z^2 +h\hat{k}_z^4+i\hat{k}_x\hat{k}_y+j\hat{k}_x^3\hat{k}_y+l\hat{k}_x\hat{k}_y^3+m\hat{k}_x^2\hat{k}_y^2 , \quad (2)$$

where

$$\hat{k}=k/\kappa , \quad \kappa=(V_F/\hat{V}_F)^{1/3} , \quad E(k)=E_F\hat{E}(\hat{k}) . \quad (3)$$

k is analogous to the Fermi wave vector for a single spherical band and E_F is the Fermi energy at zero temperature. $V_F=4\pi^3 n_h$ denotes the volume of the Fermi body containing n_h (hole) carriers and $\hat{V}_F$ is the volume of the dimensionless Fermi body enclosed by $\hat{E}(\hat{k})=1$. For convenience, we define a Fermi-energy effective mass m_F^* by

$$E_F=(\hbar\kappa)^2/2m_F^* . \quad (4)$$

Equation (2) contains all second-order terms and a selected set of fourth-order terms which are sufficient to describe the measured asymmetric shape of the hole Fermi body. Terms $k_x^2k_y^2$, $k_y^2k_z^2$, and $k_xk_yk_z^2$ have been left out, however, because their parameters could not be fixed by the available data. The sixth-order terms k_x^6 and k_y^6 have been included for stability reasons. Otherwise, $E(k)$ may take on large negative values along certain directions in k integration. Coefficients $a, b, \ldots, m, E_F$ have been fitted to the shape of the Fermi surface (see Fig. 1), the hole concentration n_h, and the cyclotron masses m^*:

$$m^*/m_0=\frac{1}{\pi}\oint\frac{d\hat{k}}{|\hat{v}_\perp|} . \quad (5)$$

Contour C is the extremal orbit perpendicular to B and $\hat{v}_\perp$ denotes (in dimensionless form) the component of the respective velocity:

$$\hat{v}(\hat{k})=\nabla\hat{E}(\hat{k}) . \quad (6)$$

Numerical results for the band parameters are listed in Table I. As expected, the Fermi energy is slightly smaller for the monoclinic band than in an ellipsoidal approximation.[4]

In kinetic theory,[5] the zero-field conductivity and the Hall tensor are directly related to the band structure,

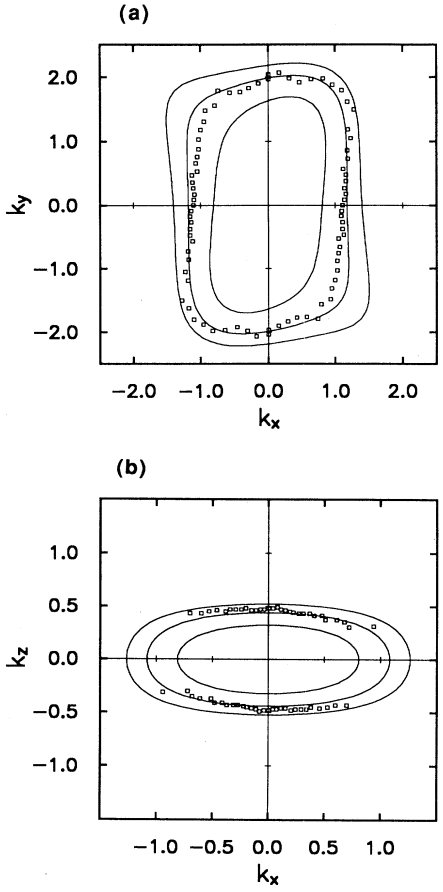

FIG. 1. Cross sections of the Fermi bodies. (a) (001) plane, (b) (010) plane. The square symbols represent the experimental data derived from SdH measurements (Ref. 4). The solid lines are calculated for different parameter sets from Eq. (2) with $\hat{E}(\hat{k})=1$.

scattering time τ, and charge q of the carriers by

$$\sigma_{ij}=\frac{q^2n\tau}{m_F^*}\hat{\sigma}_{ij} , \quad (7)$$

$$\sigma_{ijk}=\frac{q^3n\tau^2}{m_F^*}\hat{\sigma}_{ijk} , \quad (8)$$

$$\hat{\sigma}_{ij}=\frac{1}{2\hat{V}_F}\int\hat{v}_1\hat{v}_jf'(\hat{E}_{\hat{k}}-\hat{\mu})d^3\hat{k} , \quad (9)$$

$$\hat{\sigma}_{ijk}=\varepsilon_{mnk}\frac{1}{4\hat{V}_F}\int\hat{v}_i\hat{v}_n\frac{\partial\hat{v}_j}{\partial\hat{k}_m}f'(\hat{E}_{\hat{k}}-\hat{\mu})d^3\hat{k} . \quad (10)$$

TABLE I. Monoclinic hole band parameters (two equivalent pockets).

$a=0.66$	$e=0.035$	$i=-0.29$	$\hat{V}_F=5.066$
$b=0.14$	$f=0.01$	$j=0.23$	$E_F=10$ meV
$c=0.02$	$g=4.4$	$l=0.00$	$\kappa=2.037\times10^6$ cm^{-3}
$d=0.021$	$h=4.0$	$m=-0.05$	$m_F^*/m_0=0.161$

$n=n(T=0)$ is the concentration at zero temperature and $\hat{v}=\hat{v}(\hat{k})$ according to (6). $f'(\hat{E}_k-\hat{\mu})$ denotes (in dimensionless form) the derivative of the equilibrium Fermi function of the carriers with chemical potential μ. τ has been assumed independent of k, ε_{mnk} is the antisymmetric rank-three unit tensor, and the integration is over the Brillouin zone. For a single spherical band m_F^* is identical with the usual effective mass, $\hat{V}_F=(4\pi/3)$, and therefore $\hat{\sigma}_{ij}=\delta_{ij}$, and $\hat{\sigma}_{ijk}=\varepsilon_{ijk}$. At zero temperature Eqs. (9) and (10) can be reduced to integrations over the Fermi surface:

$$\hat{\sigma}_{ij}=\frac{\nu}{2\hat{V}_F}\int\frac{\hat{v}_i\hat{v}_j}{|\hat{v}|}d\hat{S}\ , \tag{11}$$

$$\hat{\sigma}_{ijk}=\varepsilon_{mnk}\frac{\nu}{4\hat{V}_F}\int\frac{\hat{v}_i\hat{v}_n\partial\hat{v}_j}{|\hat{v}|\partial\hat{k}_m}d\hat{S}\ . \tag{12}$$

$\nu(=2)$ denotes the number of equivalent Fermi bodies. To evaluate these integrals, we first solved $\hat{E}(\hat{k})=1$ for $\hat{k}_z=F(\hat{k}_x,\hat{k}_y)$ and then performed the integrations numerically.[7]

The resistivity tensor ρ_{ij} is obtained by inversion of the tensor σ_{ij} and the Hall resistivity tensor is given by

$$\rho_{ijk}=-\rho_{im}\rho_{jn}\sigma_{mnk}\ . \tag{13}$$

Summation over repeated indices is implied. In particular, the longitudinal Hall resistivity components are

$$\rho_{131}=\rho_{33}(-\rho_{11}\sigma_{131}+\rho_{12}\sigma_{321})\ , \tag{14}$$

$$\rho_{232}=\rho_{33}(-\rho_{22}\sigma_{232}+\rho_{12}\sigma_{132})\ . \tag{15}$$

Note that there are two different sources of the LHE (as described by a resistivity tensor) originating from the longitudinal Hall conductivity and the nondiagonal resistivity components. Both contributions have the same origin and tend to compensate each other.

Numerical calculations have been performed for a single monoclinic hole band as described by Eq. (2), a monoclinic hole band plus an ellipsoidal electron band, and ellipsoidal bands for both holes and electrons. Parameters have been chosen to fit the experimental resistivity and Hall resistivity data of Ref. 2 (cf. Tables II and III). A scattering time $\tau_h=2.29\times10^{-12}$ s has been used for the monoclinic hole band ($T=0$). The Hall resistivity tensor is independent of τ_h. The transverse Hall coefficients are slightly smaller than $1/n_he=9.05$. For the special form of (2), with no coupling between k_x, k_y, and k_z, we have

TABLE II. Conductivity and resistivity tensor at $T=0$: (a) monoclinic hole band, (b) hole plus electron band, (c) ellipsoidal hole and electron band. $\dot{\rho}_{ij}$ is in $10^{-4}\,\Omega$ cm.

i,j	(a) $\hat{\sigma}_{ij}$	(a) ρ_{ij}	(b) ρ_{ij}	(c) ρ_{ij}	Expt. ρ_{ij}
1,1	1.98	3.62	5.8	5.16	5.22
1,2	−0.11	0.41	−1.0	3.86	?
2,2	0.91	7.92	5.3	5.99	4.5–7.4
3,3	11.00	0.65	1.0	1.21	1.0–1.42

$$\hat{\sigma}_{131}=\hat{\sigma}_{232}=\tfrac{1}{2}\hat{\sigma}_{12}\left\langle\frac{\partial\hat{v}_3}{\hat{k}_3}\right\rangle\ , \tag{16}$$

where $\langle\ \rangle=2g+12h\langle k_z^2\rangle=11.7$ denotes an average over the Fermi surface. Comparison with the experimental data (Table III) shows that the LHE elements are much too small. In addition, two out of three THE elements even have a wrong sign.

The negative signs of ρ_{213} and ρ_{321} indicate an important electronic contribution to the Hall effect so that a single monoclinic hole band cannot account for the observed THE. As a first approximation for the electron band, we assume an ellipsoidal shape with principal axes not being parallel to the k_x, k_y, and k_z axes and take the orientation and the effective masses as fitting parameters, $m_i^*=\hat{m}_i m_e^*$ with $\hat{m}_1\hat{m}_2\hat{m}_3=1$. The mean electron effective mass $m_e^*=0.02m_0$ represents a typical value for a semimetal. With respect to the principal axes we have

$$\hat{\sigma}_{ij}^e=\frac{1}{\hat{m}_i}\frac{n_e(T)}{n_e(0)}\delta_{ij}\ ,\quad \hat{\sigma}_{ijk}^e=\frac{1}{\hat{m}_i\hat{m}_j}\frac{n_e(T)}{n_e(0)}\varepsilon_{ijk} \tag{17}$$

[no summation on index i on the right-hand side of (17)]. Then, the electronic conductivity and Hall tensor contributions were rotated around the k_3 axis by an angle ϕ:

$$\hat{\sigma}_{ij}=R_{il}R_{jm}\hat{\sigma}_{lm}^e\ ,\quad \hat{\sigma}_{ijk}=R_{il}R_{jm}R_{kn}\hat{\sigma}_{lmn}^e\ , \tag{18}$$

where R_{il} denotes the corresponding rotation matrix. A reasonable fit of the experimental data was obtained for $\hat{m}_1=7$, $\hat{m}_2=0.35$, $\hat{m}_3=0.408$, $\phi=20°$, $\tau_h=1.3\times10^{-12}$ s, and $\tau_e/\tau_h=1.9$; see Tables II and III.

Although the results of the previous section are in reasonable agreement with experiment, they are not yet physically acceptable. In particular, no choice of the

TABLE III. Hall tensor at $T=0$: (a) monoclinic hole band, (b) hole plus electron band, (c) ellipsoidal hole and electron band: ρ_{ijk} is in cm^3/As.

i,j,k	(a) $\hat{\sigma}_{ijk}$	(a) ρ_{ijk}	(b) ρ_{ijk}	(c) ρ_{ijk}	Expt. ρ_{ijk}
2,1,3	−0.85	8.37	−10.0	−9.32	−9.2
1,3,2	−10.71	8.86	2.4	12.29	12.3
3,2,1	−4.81	8.69	−30.0	−29.20	−29.1
1,3,1	−0.63	0.07	7.6	11.62	11.6
2,3,2	0.63	−0.13	−12.5	17.52	17.4

TABLE IV. Hole and electron conductivities [in $(\Omega\,\mathrm{cm})^{-1}$] of the ellipsoidal band model at $T=0$.

i,j	Holes σ_{ij}	Electrons σ_{ij}
1,1	3133	605
1,2	−1368	−1039
2,2	1161	2059
3,3	7591	681

(electron) parameters leads to ρ_{131}, and ρ_{232} being positive and of correct magnitude. The reason is, probably, the rather small hole contribution to σ_{12}, σ_{131}, and σ_{232} within the monoclinic band model. To overcome this shortcoming, we tried an ellipsoidal band model for both holes and electrons. For each band the rotated tensor elements are given by

$$\hat{\sigma}_{11}=\cos^2\phi\hat{\sigma}'_{11}+\sin^2\phi\hat{\sigma}'_{22}\ , \tag{19}$$

$$\hat{\sigma}_{12}=\sin\phi\cos\phi(\hat{\sigma}'_{22}-\hat{\sigma}'_{11})\ , \tag{20}$$

$$\hat{\sigma}_{22}=\sin^2\phi\sigma'_{11}+\cos^2\phi\hat{\sigma}'_{22}\ , \tag{21}$$

$$\hat{\sigma}_{33}=\hat{\sigma}'_{33}\ , \tag{22}$$

$$\hat{\sigma}_{213}=-\hat{\sigma}_{11}\hat{\sigma}_{22}+\hat{\sigma}_{12}^2\ , \tag{23}$$

$$\hat{\sigma}_{132}=-\hat{\sigma}_{33}\hat{\sigma}_{11}\ , \tag{24}$$

$$\hat{\sigma}_{321}=-\hat{\sigma}_{33}\hat{\sigma}_{22}\ , \tag{25}$$

$$\hat{\sigma}_{131}=\hat{\sigma}_{33}\hat{\sigma}_{12}\ , \tag{26}$$

$$\hat{\sigma}_{232}=-\hat{\sigma}_{33}\hat{\sigma}_{12}\ . \tag{27}$$

For a single band this [by Eq. (13)] leads to

$$\rho_{ijk}=-\frac{1}{nq}\varepsilon_{ijk} \tag{28}$$

being identical with the spherical band result. In particular, there are no longitudinal Hall resistivity components. For the case of a hole and an electron band, contributions (19)–(27) are added with the appropriate prefactors [see Eqs. (7) and (8)]. This procedure reproduces Eq. (22) of Ref. 2 for ρ_{232}. The conductivity parameters, four each for the hole and electrons, are fitted to the eight measured resistivity and Hall resistivity components for $T\to 0$ (Tables II–IV). This can be done almost perfectly, and, moreover, the fitted conductivity components represent positive-definite tensors and the effective-mass ratios ($m^*_{h2'}/m^*_{h3'}\approx 16$) for the hole band are at least in qualitative agreement with the Fermi-surface data.[4] An even larger anisotropy ($m^*_{e1'}/m^*_{e2'}\approx 40$) results for the electron band, which is, of course, inconsistent with the original determination of n_e. The surprising success of the ellipsoidal two-band model clearly suggests a critical revision of the earlier interpretation of the SdH data. The corresponding rotation angles are $\phi_h=27.1°$ and $\phi_e=-27.5°$. We note that ϕ_h is close to the angle between the k_x axis and the longer diagonal of the Fermi-surface cross section (see Fig. 1).

Our theoretical investigations can be summarized as follows. Within a single monoclinic band no satisfactory description of the experimental Hall data could be obtained. In particular, the longitudinal components are much too small. It seems that a significant LHE cannot result from a single band. For the ellipsoidal two-band model, however, a perfect agreement is obtained using reasonable assumptions for hole and electron densities. Moreover, the orientation and anisotropies of the hole and electron ellipsoids can be determined. We conclude that a significant LHE is not produced by a single low-symmetry band. The real origin lies in the fact that the low symmetry allows for the existence of two quasiellipsoidal bands whose principal axes are rotated with respect to each other. As a next step in our theoretical investigation of the LHE we have to include the magnetoresistivity data to obtain a self-consistent determination of the hole and electron concentrations n_h and n_e. Then, realistic temperature dependencies for carrier concentrations and mobilities should be built in to reproduce the measured temperature variations of the transport coefficients. For trigonal α-arsenic the first mentioned procedure has been successfully performed in an earlier paper by Jeavons and Saunders.[8] However, the point group $\bar{3}m$ of α-As does not allow for longitudinal Hall coefficients.

[1]M. Möllendorf and W. Bauhofer, Phys. Rev. B **30**, 1099 (1984).
[2]W. Bauhofer, Phys. Rev. B **32**, 1183 (1985).
[3]W. Bauhofer, Phys. Rev. B **38**, 5215 (1988).
[4]B. L. Zhou, E. Gmelin, and W. Bauhofer, Solid State Commun. **51**, 757 (1984).
[5]A. C. Smith, J. F. Janak, and R. B. Adler, *Electronic Conduction in Solids* (McGraw-Hill, New York, 1964).
[6]R. R. Birss, *Symmetry and Magnetism* (North-Holland, Amsterdam, 1964).
[7]W. H. Press, B. P. Flannery, S. A. Teukolsky, and W. T. Vetterling, *Numerical Recipes* (Cambridge University, Cambridge, 1986).
[8]A. P. Jeavons and G. A. Saunders, Proc. R. Soc. London, Ser. A **310**, 415 (1969).